Eyesafe high peak power pulsed fiber lasers limited by fiber nonlinearity

Guillaume Canat, Williams Renard, Erik Lucas, L. Lombard, J. Le Gouët, Anne Durecu, P. Bourdon, Sylvain Bordais, Yves Jaouën

Eyesafe high peak power pulsed fiber lasers limited by fiber nonlinearity

G. Canat [a,*], W. Renard [a], E. Lucas [b], L. Lombard [a], J. Le Gouët [a], A. Durécu [a], P. Bourdon [a], S. Bordais [b], Y. Jaouën [c]

[a] Onera – The French Aerospace Lab, 91123 Palaiseau, France
[b] Keopsys, 2 rue Paul Sabatier, 22300 Lannion, France
[c] Telecom Paristech, CNRS/LTCI UMR5141, 46 rue Barrault, 75634 Paris, France

We present design and performances of several eye-safe high peak power fiber lasers operating either around 1550 nm or 2000 nm. They share the limitations by nonlinear effects either Stimulated Brillouin Scattering for single frequency lasers or Kerr related effects for short pulse amplifiers. Performances above 1 kW peak power for single frequency lasers and 26 nJ for short pulse fiber lasers are reported. The influence of the saturation power of the fibers on the non-linearity is discussed and applied to a comparison between Erbium and Ytterbium co-doped fibers and Thulium doped fibers. The Brillouin gain properties in these fibers are also compared.

1. Introduction

Coherent wind LIDARs are increasingly used for climatic condition and turbulence assessment with applications in wind farm projects optimization or aircraft security during take-off and landing. Laser pulses are sent through the atmosphere and wind speed is measured using Doppler-induced frequency shift on the backscattered laser light. Laser sources with excellent spatial beam quality, narrow linewidth and typical pulse duration ranging from ~100 ns to 1 μs are required.

Gas detection by spectral absorption in MWIR (3–8 μm) and LWIR (8–15 μm) bands address many applications both in civil and military areas. For example monitoring of air quality, detection of gas leaks in industrial environment or detection of explosive gasses can be addressed by infrared Optical Parametric Oscillators (OPOs). Again, pulsed laser sources with excellent beam quality and narrow linewidth (for OPOs operated in the single longitudinal mode regime) are required.

However, narrow linewidth pulsed Master Oscillator Power Fiber Amplifier (MOPFA) are usually limited in peak power by nonlinear effects arising in the fiber such as Stimulated Brillouin Scattering (SBS) to a few 10–100s Watts in standard fibers [1]. Strategies can be used to mitigate nonlinear effects: for example, shortening the amplifying fiber or counter pumping. However, those strategies may have an impact on amplifier efficiency or complexity. Higher doping levels increases the available amplifying gain per meter but new limits appear like parasitic lasing effect at 1 μm in Er^{3+}:Yb^{3+}-doped fibers [2,3] and cross-relaxations/upconversion effects in Tm^{3+}-doped fibers leading to higher level populating [4] and photodarkening [5].

A careful design of the amplifier architecture is required to balance the amplifier performances and nonlinear effects mitigation strategies. This paper deals with the designs of 1.5 and 2 μm narrow linewidth pulsed MOPFA optimized for peak power and efficiency.

Pulsed MOPFA at 1.5 μm and 2 μm are well-adapted and versatile sources. They offer frequency tunability, narrow linewidth and good beam quality as well as compactness and robustness. As can be seen on Fig. 1, accurate setting of master oscillator wavelength is useful to avoid absorption peaks in the atmosphere.

In this paper we report on different MOPFA configurations generating pulses with high peak power at l.5 μm and 2 μm, respectively. It is well-known that nonlinear effects such as the optical Kerr effect, Stimulated Raman Scattering (SRS) and SBS can be observed in optical fibers [6]. We introduce an intensity length product parameter to quantify the importance of nonlinear effects in MOFPA. Sections 3 and 4 describe the obtained performances of narrow linewidth high peak power MOPFAs limited by SBS effect at 1545 nm and 2050 nm, respectively. Section 5 describes a short pulse MOPFA emitting at 1960 nm which the propagation of short pulses can be associated with pulse broadening induced by Kerr effect: the Self-Phase-Modulation (SPM). Section 6 analyzes the evolution of the effective length involved in the intensity length product with amplifier gain and saturation. Erbium–Ytterbium co-doped and Thulium doped fibers are

* Corresponding author.
E-mail address: guillaume.canat@onera.fr (G. Canat).

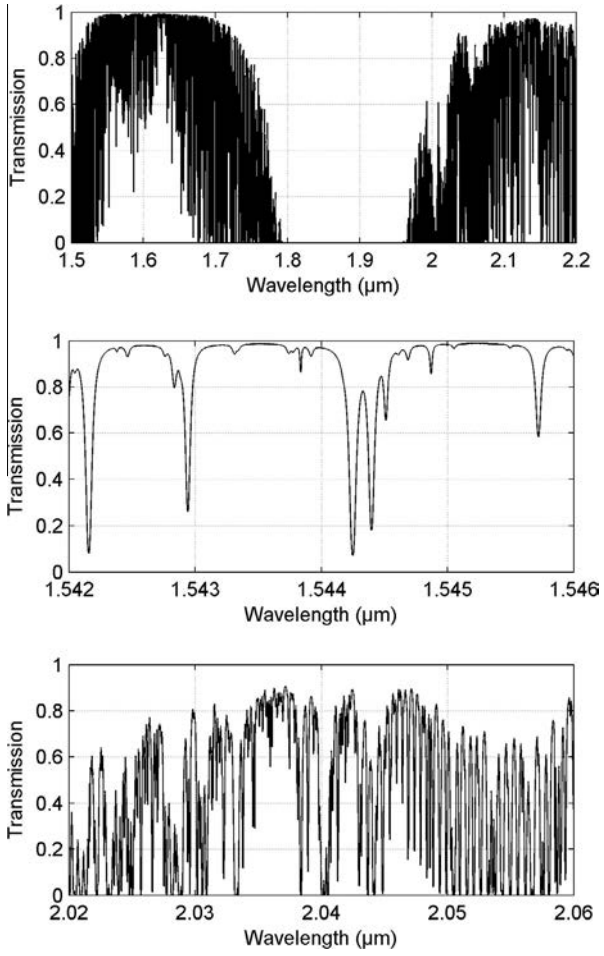

Fig. 1. Atmospheric transmission of a 10 km horizontal path on ground (standard atmosphere, no aerosol). Top: 1.5–2.2 μm transmission, middle: 5 nm zoom around 1.54 μm, bottom: 5 nm zoom around 2.04 μm.

compared with this respect. Section 7 finally compares the Brillouin gain properties of these fibers.

2. Theory of nonlinearities in fiber amplifiers

Nonlinear effects such as SPM, SRS and SBS can be observed in high power amplifiers as short as a few meters. The strength of the nonlinearities in a fiber can be quantified by the intensity length product:

$$B = g\frac{\int_0^L P(z)dz}{A_{eff}} = \frac{gP(L)L_{eff}}{A_{eff}} \quad (1)$$

where g is a nonlinear gain, L is the fiber length, A_{eff} is the effective area, $P(z)$ is the power distribution along the fiber, L_{eff} is the effective length. For passive fiber the effective length is equal to the fiber length and for active fiber the effective length depends on the fiber gain along the fiber [6]. This equation applies for SBS, SRS and SPM using corresponding gains.

When considering the SBS, g is the Brillouin gain g_{B}. In single-mode fibers, the SBS threshold is reached when the peak power time length product reaches about 80 Wm. The high power density generates acoustic waves into the fiber core which acts as a grating. The light transmitted by the fiber saturates and part of this light is backscattered by the grating [7]. In fiber amplifiers, the backscattered light may be amplified into the active fiber generating high peak power backscattered pulses potentially harmful for beforehand components [8]. When considering the SRS, g is the Raman gain g_{R}. When considering the SPM, B is usually referred for short pulse systems as the B-integral and quantifies the pulse nonlinear phase shift [9]. In that case:

$$g = \frac{2\pi n_2}{\lambda} \quad (2)$$

with n_2 the nonlinear refractive index.

From (1) it appears that there are three ways to act on the nonlinearities. First the effective area can be increased. Large-Mode-Area (LMA) fibers, with large core diameter and low numerical aperture (NA) may be used to increase the mode area but the fiber tends to guide higher order transverse modes degrading the beam quality. A good spatial quality is crucial for many applications. For instance in a coherent detection Lidar when M^2 equals to 1.73 we expect the Carrier-to-Noise Ratio (CNR) to decrease by 3 dB [10]. In order to stay in the effectively single-mode limit, the normalized frequency must be kept lower than 2.405 to keep the fiber single-mode. Actually the fiber can still produce good beam quality for NA 0.09 and $V \sim 4$–5 provided that the injection is carefully controlled. At 1545 nm the maximum core diameter is 25 μm for $V = 4.5$. Due to the wavelength dependence of V the maximum core diameter at 2050 nm increases to 33 μm. In this way, the corresponding effective area increases from 327 μm^2 to 570 μm^2.

Second way to decrease B is to minimize the integral of the power over the fiber length. This term also equals by definition to the product of fiber output power times effective length L_{eff}. This will be discussed in Section 6.

Last way to decrease B is to decrease the nonlinear gain. This can be done by tuning the dopants in the fiber. For example, the nonlinear index n_2 is lower in aluminosilicate glass compared to phosphosilicate glass [6,11]. The Brillouin nonlinear gain coefficient is supposed to be comparable for both glasses although no direct measurement allowing comparison has been performed to date. This will be discussed in Section 6. Another way to decrease the effective Brillouin gain g_{B} is to broaden the g_{B} spectrum. This can be done by fiber structure engineering or applying temperature or strain gradient along the fiber. Experimental results are reported in Sections 3–5 using this last technique.

3. High peak power narrow linewidth MOPFA emitting at 1545 nm

Due to the high reliability of fiber lasers, single-frequency linearly polarized pulsed MOPFA are used for coherent Doppler wind-lidar applications [10]. With the development of efficient and reliable photonic components developed for optical communication systems at 1.5 μm and low atmospheric absorption near this wavelength, narrow linewidth MOPFA near 1.5 μm are suitable for these applications. Erbium doped fibers may be used as gain medium but lasers and amplifiers are limited to about 1 W average power with low efficiency due to low absorption and low achievable Erbium ions concentration into the fiber core. Erbium–Ytterbium co-doped fibers have enabled power scaling of 1.5 μm fiber lasers in CW and pulsed regime due to high absorption of Ytterbium ions and energy transfer between Ytterbium and Erbium ions. For coherent wind-lidar application the master oscillator has to be narrow linewidth (<1 MHz) in order to have a good accuracy for the wind speed measurement. The pulse energy is then limited in peak power by SBS. Many teams are still working on increasing the SBS threshold in order to extract more energy and power of narrow linewidth fiber laser systems.

LMA fibers enable high peak power generation while maintaining good spatial quality. Onera has used 40 μm core diameter multifilament-core fibers (MFC) to amplify high peak power pulses

[12]. Pulses with 940 W peak power, 1 μs duration and 1 MHz laser linewidth were achieved. The beam quality is good with M^2 ~1.3. This laser setup is nevertheless not all-fiber. Shi et al. tried to increase the SBS threshold with the use of an LMA Er^{3+}–Yb^{3+}-doped phosphate glass fibers [13]. The main advantage of phosphate glass fiber is the high rare-earth doping concentration that can be reached (typically one order of magnitude higher than in silica) allowing to significantly reduce the fiber length. Besides with this glass, low NA with rare-earth doped fiber are possible, typically less than 0.06. Large core diameter (typically up to 30 μm) with a single-mode emission is thus possible. However the optical efficiency of phosphate glass fiber amplifiers seems significantly lower compared to efficiency of silica glass fiber amplifiers. In Ref. [13], the slope efficiency achieved is 4.2% at 1530 nm and 1.5% at 1572 nm with respect to the injected pump power. MFC and phosphate-glass fiber fabrication and integration in all-fiber lasers systems are challenging. With standard LMA silica based fibers, external SBS mitigation techniques have been demonstrated. A strain gradient [14] or temperature gradient [11] 43 can be applied along the fiber to broaden the SBS gain spectrum. Recently, Zhang et al. [15] achieved kilowatt peak power 500 ns duration pulses at 10 kHz Pulse-Repetition-Frequency (PRF). To overcome the SBS threshold a strain gradient along the LMA Er^{3+}–Yb^{3+} doped fiber was applied [14]. Fibertek reached with an undisclosed proprietary technique 700 W peak power 560 μJ energy pulses with 800 ns duration at 25 kHz PRF [16]. The pulse energy was limited by the available pump power and can be increased by reducing the PRF or increasing the available pump power.

We have recently developed a high power single-frequency all-fiber MOPFA using high reliability passive components. This MOPFA was used in the first experimental demonstration of a fiber laser based wind lidar with more than 10 km range [17]. The experimental setup for the pulsed fiber laser is shown in Fig. 2. All the setup is based on polarization maintaining components. A continuous-wave (CW) single-frequency laser diode or fiber laser is used as master oscillator. This source emits at a wavelength of 1545.33 nm which corresponds to high gain in erbium doped fibers and a good atmospheric transmission. An Acousto-Optic-Modulator (AOM) is used to modulate the CW signal from the seed laser. A commercially available preamplifier scales the energy of pulses up to the SBS limit in the single-mode fibers. A band-pass filter and isolator is inserted before the last high power amplifier stage to suppress the Amplified Spontaneous Emission (ASE) from previous amplifier stage. A home-made mode-field-adapter (MFA) is used to excite the fundamental-mode of the LMA fibers used in the booster. To increase the SBS threshold we used LMA fibers with larger mode-field-diameter (MFD). It turns out that in order to have the best energy transfer between Ytterbium and Erbium ions, the active fiber is co-doped with phosphorus [18]. For the targeted application it is important to have a good beam quality, characterized with an $M^2 < 1.7$ [10]. This co-dopant increases the fiber core refractive index and fiber NA. Finally, the power amplifier stage is based on a PM Erbium–Ytterbium co-doped LMA fiber with 25 μm core diameter. This fiber was pumped with 30 W of 975 nm laser diodes. The fiber length was 1.8 m. The signal and pump light are coupled into the core and the pump cladding respectively with a commercial pump combiner.

The signal amplitude modulation applied with the AOM is optimized to have a Gaussian-like pulse at the laser output. Indeed, the pulse shape changes after amplification because of gain saturation [19]. SBS limits the pulse peak power to 300 W. The corresponding energy and pulse duration are 200 μJ and 600 ns, respectively with 10 kHz PRF (Fig. 3). The M^2 is measured to be less than 1.3 in both axes. The Polarization-Extinction-Ratio (PER) is better than 17 dB.

In a second step, in order to increase the SBS threshold of the power amplification stage a strain gradient was applied to the doped fiber to decrease the effective length. Peak power up to 470 W was achieved with 850 ns pulses (Fig. 5) and 400 μJ energy (Fig. 4). With shortest pulse duration, peak power up to 630 W was achieved with 550 ns pulses. The output peak power was then increased by 3.2 dB and limited by the available pump power.

4. High peak power narrow linewidth MOPFA emitting at 2050 nm

For more than 10 years Thulium doped fiber lasers have progressed with the demonstration of high power and highly efficient fiber lasers and amplifiers. Jackson et al. worked on silica fiber composition in order to enhance the cross-relaxation effect (or 2 for 1) which allows efficient pumping with laser diodes around 793 nm [4]. Most of the work was focused in the 1900–2000 nm emission band of Tm^{3+}-doped fibers in CW or pulsed regime. For example, in pulsed single-frequency regime, up to 500 μJ energy and 33 kW peak power with 15 ns pulses were achieved at 1918 nm [20]. In this regime the pulse duration is comparable with the phonon lifetime and the SBS threshold is strongly increased. With 80 ns pulse duration, 220 μJ and 2.75 kW peak power were achieved from a single-frequency Q-switched MOPFA using germanate-glass fibers [21]. But for many applications, single-frequency, linearly polarized fiber lasers operating in the wavelength range of 2.0–2.1 μm have to be developed. Goodno et al. reported the highest power at 2040 nm with 608 W in CW regime [22]. These wavelengths correspond to the first atmospheric transparency window and eye-safe range that are highly desirable for many applications, such as LIDARs or pumping of OPOs based on ZGP or Op-GaAs [23,24]. Operating high peak power fiber amplifiers in the 2.02.1 μm band is more difficult due to the

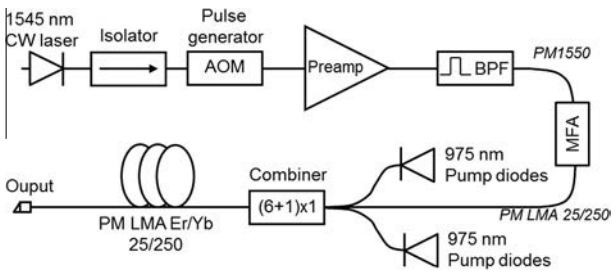

Fig. 2. Experimental setup. CW, continuous-wave; AOM, acousto-optic-modulator; BPF, bandpass-filter; MFA, mode-field-adapter.

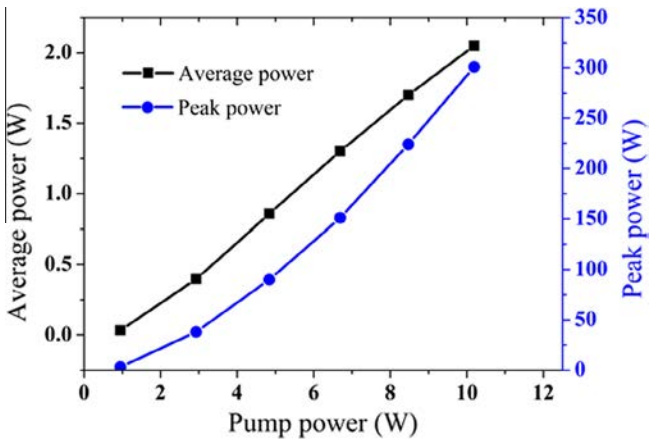

Fig. 3. Average power and peak power vs. pump power in the power amplifier stage. SBS limits the extractable energy.

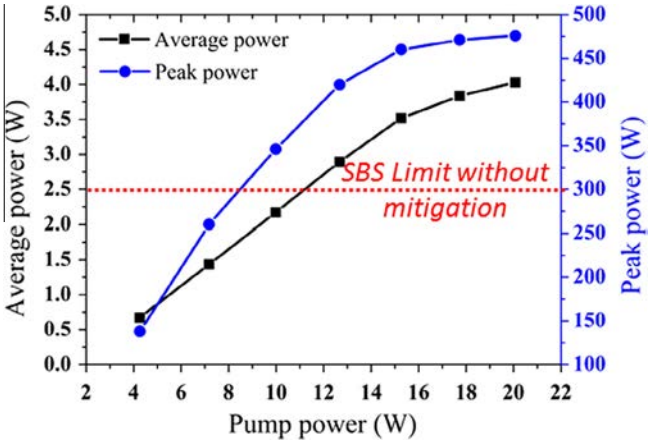

Fig. 4. Average power and peak power vs. pump power in the power amplification stage with our SBS mitigation system.

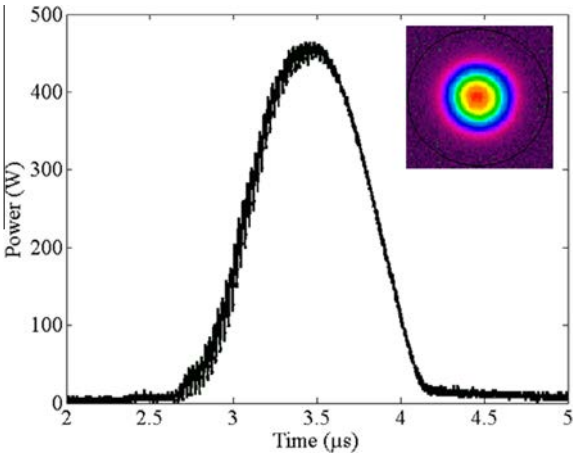

Fig. 5. Pulse shape (about 850 ns) at the highest energy (400 μJ energy, 470 W peak power) and beam profile.

low gain per meter of Tm^{3+} doped fibers. There are some similarities with the *L* band for Erbium doped fiber in this situation. The use of longer fibers lowers the nonlinearity threshold.

We developed a high power single-frequency laser source at 2050 nm using strain gradient to mitigate SBS [25]. The pumping scheme selected for the amplifier is clad pumping using 793 nm laser diodes. Other pumping schemes are possible like core pumping with 1550 nm Er^{3+}-doped fiber laser [26] or Tm^{3+}-doped fiber in the 1.8–1.9 μm range [27]. Core pumping using a Tm^{3+}-doped fiber laser in the 1.8–1.9 μm range is particularly interesting as the optical efficiency when pumping at these wavelengths can reach up to 93% but it results in a more complex system whose total efficiency is lower. The 793 nm multimode diode pumping can result in up to 60% efficiency in CW laser thanks to cross-relaxation [12,28]. The MOPFA layout is shown Fig. 6. It consists in three amplification stages.

A linearly polarized Distributed Feedback laser (DFB) emitting a power of 4 mW with <4 MHz linewidth at 2050 nm is coupled into a 24 dB gain fiber amplifier to boost the laser power to 1 W CW (OSNR > 40 dB) with a 6 μm core diameter PM, double clad, Tm^{3+}-doped fiber cladding pumped at 793 nm. The seed is modulated into pulses from 100 ns to 400 ns, 320 mW peak power using a fiber AOM. Pulses are then injected into the second amplification stage. This amplifier is built with a 10 μm core diameter PM, double clad, Tm^{3+}-doped fiber backward cladding pumped. The second stage output is limited by pump power to a maximum of 23 dB gain and 70 W peak power.

To prevent third amplification stage saturation with ASE of the second stage, a band-pass filter is added. The third amplifier is built using a PM, LMA, double clad, Tm^{3+} highly doped fiber with 25 μm core diameter 0.09 NA. The amplifier is spliced to matched passive fibers on both ends. The fiber is slightly multimode with a normalized frequency of $V = 3.44$. It is cladding-pumped in forward direction by 793 nm laser diodes. The amplifier output is collimated and passes through a free space isolator providing 28 dB isolation. Beam quality was measured using a ModeScan and a 25 μm slit PYROCAM and the $M^2 = 1.2$ on both axes. The far field beam shape is shown on Fig. 7. We observed no dependence of M^2 on pump power. As shown on Fig. 7, the SBS threshold was reached in this configuration at 535 W output peak power for 17 W pump power. The pulses generated have 110 ns duration with 20 kHz repetition rate.

A patent pending SBS mitigation system which implements a triangular strain gradient in the fiber was then used on the third amplification stage. Thanks to this system we reached 1 kW peak power, 110 ns pulses, 20 kHz PRF, for 20 W of pump power. The maximum peak power is thus increased by 3 dB compared to the unstrained case. Fig. 8 presents the peak power as a function of the pump power, for different pulse durations. The power is limited by SBS for 100–270 ns pulses. For longer pulses, it is the available pump power which limits the maximum achievable peak power.

5. Amplification of ultrashort pulses in Tm^{3+}-doped single-mode fiber amplifier at 1960 nm

Nonlinearities in fibers limit the peak power of pulses. SBS first occurs with single-frequency lasers for pulse duration longer than the phonon lifetime (i.e., >15 ns) while SPM limits pulse energy and peak power of ultrashort pulses (<10 ps). For ultrashort pulses, the fiber dispersion (linear) and SPM (nonlinear) induce chirp and change the temporal pulse shape. These effects may compensate and pulses are solitons with a quantified energy linked to their pulse duration [9].

$$E = N\frac{3.53|\beta_2|}{\gamma\tau} \tag{3}$$

with *E* the soliton energy, *N* the soliton order, β_2 the second order dispersion, γ the nonlinear parameter and τ the soliton duration. The second order dispersion of standard fibers at 2 μm is about $-80\ ps^2/m$ [29]. The nonlinear parameter, linked to the nonlinear

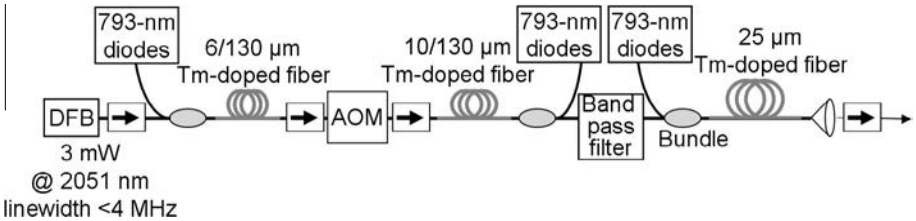

Fig. 6. Three stages amplifier layout. AOM, acousto-optic modulator.

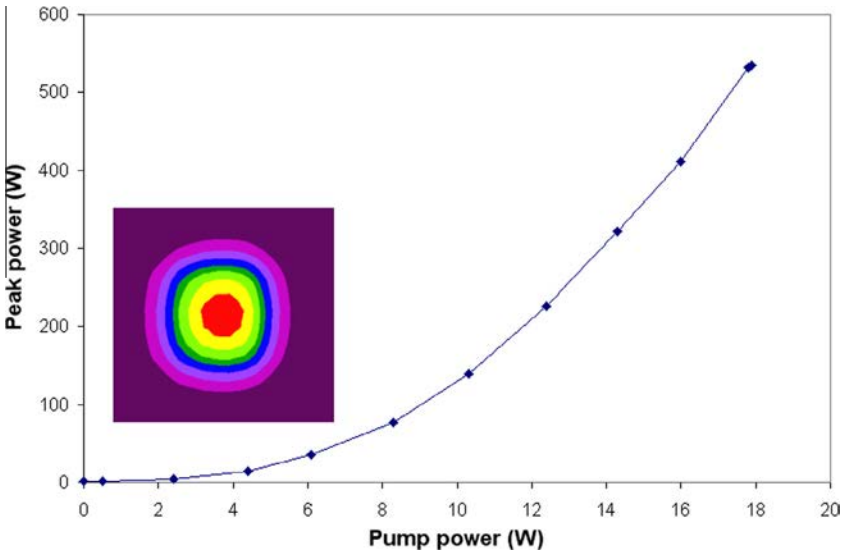

Fig. 7. Third stage output peak power as a function of launched pump power. Inset: far field beam profile.

refractive index is about 2.10^{-3} W^{-1} m^{-1} for single-mode fibers at 2 μm. Then, with standard single-mode fiber the pulse energy of a fundamental soliton is limited to about 10–100 pJ for 100 fs–10 ps pulse duration respectively. This energy is not sufficient for most applications and solitons have to be amplified. For very high power amplification, chirped-pulse-amplification (CPA) is favored. But this solution needs to use free space optical components like gratings or prims. At 2 μm McComb et al. reported the first generation and direct amplification of ps pulses into a LMA Tm^{3+}-doped fiber amplifier [30]. Pulses reached 2.6 kW peak power and 13 nJ energy. The use of LMA fiber can lead to increased pulse energy with higher nonlinearities threshold but LMA fibers are slightly multimode and mode beating can appear on the output. Sims et al. [31] and Haxsen et al. [32] reached up to 150 nJ pulse energy with CPA, but the experimental setup is not all-fiber. Here we discuss the power limitation of single-mode all-fiber amplification. We consider a core-pumped Tm^{3+}-doped fiber co-propagating amplifier (Fig. 9).

For ultrashort pulse regime, we can calculate the B-integral [33] as a function of input and output energies for a constant gain volume of a single-mode Tm^{3+}-doped fiber. The B-integral defined by Eq. (1) is a parameter measuring the nonlinear phase shift. The amplification of pulses is said linear when B is smaller than $\pi/2$.

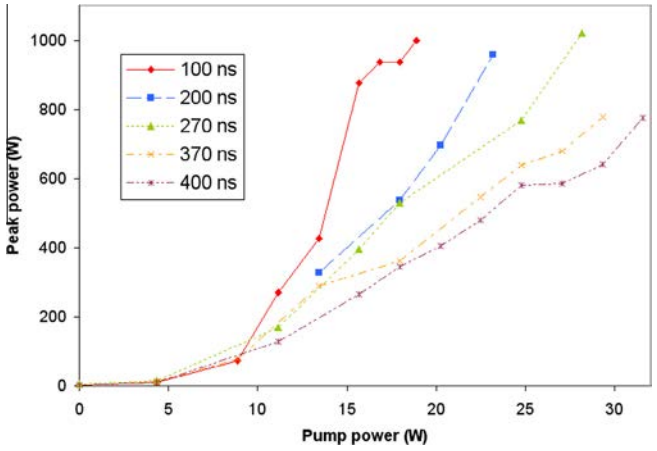

Fig. 8. Third stage output peak power as a function of pump power with SBS mitigation system for different pulse durations.

We have computed the B-integral and output pulse energy with the steady state equation for a two-levels Tm^{3+}-doped single-mode fiber steady state amplifier. Indeed, due to high PRF in mode-locked fiber lasers and low pulse energy compared to the fiber saturation energy the steady state equations can be solved. For different input energies, we changed the pump power at 1560 nm between 1 W and 5 W and the fiber length while keeping the same gain volume of the single-mode fiber. Then this model gives us the output energy and the evolution of the pulse peak power along the fiber which enables us to calculate the B-integral. We have found that the B-integral varies only with the input and output energy for a given gain volume (Fig. 10).

The best way to extract the highest energy with $B < \pi/2$ is to decrease the input energy. For our example, with 180 pJ input energy, the maximum output energy is about 17 nJ. With 4.5 pJ input energy the maximum output energy is about 35 nJ with 39 dB amplifier gain. Therefore a 3 dB increase of output energy may be reached with a well-chosen input energy. But the reduction of input power will strongly decrease the slope efficiency and increase the generation of ASE. Moreover, our numerical model did not include the cross-relaxation effects which are probably very significant for large concentration fibers at low input energy [34].

Using these ideas we amplified a mode-locked 1960 nm thulium doped fiber laser without pulse distortion. The mode-locked oscillator delivers 4.5 ps pulses at 11.2 MHz PRF. More details on the oscillator can be found on Refs. [29,35]. Picosecond pulses were amplified into a highly-doped 50 cm long Tm^{3+}-doped fiber pumped into the core by a 5 W 1560 nm fiber laser. The nonlinear phase shift reached $\pi/2$ for 26 nJ pulse energy. On Fig. 11 we can see the slight spectral broadening due to SPM.

Pulse duration of 3.5 ps was measured with an autocorrelator and the corresponding peak power is 7.4 kW.

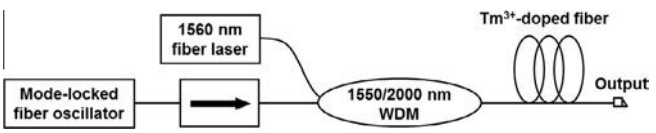

Fig. 9. Experimental setup of a core-pumped Tm^{3+}-doped fiber co-propagating amplifier.

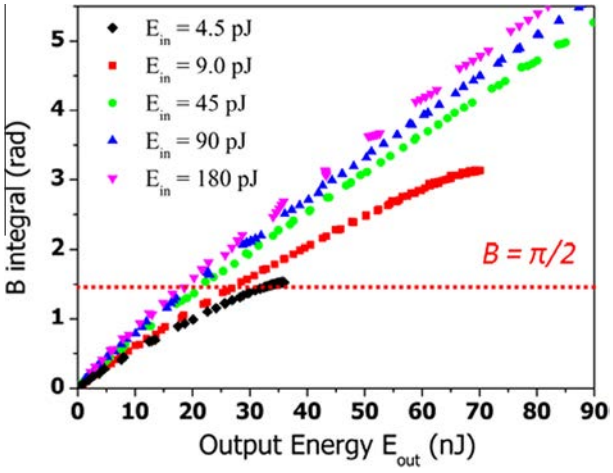

Fig. 10. Computed B-integral vs. output energy for different input power and constant small-signal absorption.

6. Influence of spectroscopy on effective length

The various examples presented in the previous sections illustrate high peak power amplifiers limited by nonlinearity. It is interesting to compare the narrow linewidth results of Sections 3 and 4. In the absence of strain based Brillouin mitigation, the peak power at the Brillouin threshold achieved is twice smaller for the short Erbium–Ytterbium co-doped fiber amplifier (1.8 m long) than for a long Thulium doped fiber amplifier (4.5 m long): 300 W and 550 W peak power, respectively. We will discuss in this section the dependence of the effective length on doping and spectroscopy that explains part of this difference. Eq. (1) shows that in order to achieve high peak power with minimum nonlinearity the effective length must thus be minimized. In an amplifier characterized by its internal gain G_A with a constant linear gain, the effective length has the analytical solution: $L_{eff} = L/\ln(G_A)$. The actual internal gain will saturate in a real fiber and the power growth along the fiber will become more linear when going toward the fiber end. We show in Appendix A that an analytical expression can be derived in the frame of a more realistic model in CW regime of a saturating two level system with constant gain and saturation power. The expression of the effective length is then given by equation:

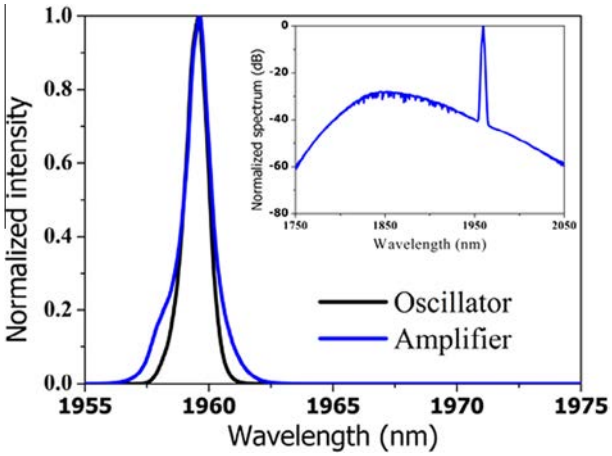

Fig. 11. Normalized optical spectra, resolution of 0.05 nm. Black line oscillator spectrum; gray line, 26 nJ amplified pulses; inset broadband optical spectrum of 26 nJ pulses. (For interpretation of the references to colour in this figure legend, the reader is referred to the web version of this article.)

$$L_{eff} = \frac{1}{g_0}\left[1 - G_A^{-1} + \frac{1 - G_A^{-2}}{2}\frac{P(L)}{P_{sat}}\right] \tag{4a}$$

In the high gain limit we find:

$$L_{eff} \approx \frac{L}{\ln G_{ss}}\left[1 + \frac{1}{2}\frac{P(L)}{P_{sat}}\right] \tag{4b}$$

where $G_{ss} = \exp(g_0 L)$ is the small signal gain, $P(L)$ is the signal power at the fiber output and P_{sat} is the fiber saturation power:

$$P_{sat} = \frac{h\upsilon_s A_{doped}}{(\sigma_a + \sigma_e)\Gamma\tau}$$

with υ_s the frequency, A_{doped} the doping area of the active fiber, σ_a and σ_e absorption and emission cross sections respectively, Γ the overlap factor and τ the transition lifetime.

Although established in CW regime and for a quasi 2 levels system this expression is helpful to understand the power growth along the fiber.

Expression (4a) admits two limits. In the first limit, when the output power is small compared to the saturation power, the effective length equals $L/\ln G_{ss}$. In the second limit, when the output power is large compared to the saturation power the limit (4b) is no longer valid and the effective length equals $L/2$ (cf. Appendix A).

We can see with this expression that in order to minimize the Brillouin gain, one wishes at the same time to maximize the linear gain per unit length and to maximize the saturation power. This calls to use highly doped fibers. One it has been selected it is interesting to consider the ratio $r = L_{eff}/L$ that characterizes the power distribution. If $P(z)$ is constant in the fiber, r is close to 1. If $P(z)$ is linearly increasing, $r = 1/2$. If $P(z)$ is exponentially increasing, $r = 1/\ln G_{ss}$ (cf. Fig. 12b).

Eqs. (4a) and (4b) show that r will increase with output power. Good efficiency requires saturation of the amplifier meaning that the power distribution $P(z)$ tends to be linear and r is closed to 0.5 or more. On the other hand the best power profile for low nonlinearity is exponential with low r value which means low saturation and reduces efficiency. This makes understand that there is a trade-off between efficiency and nonlinearity.

The first condition leads to maximize the doping concentration. However there exist several limitations to the maximum dopant concentration that can be achieved in silica. Clustering leads to inhomogeneous pair induced quenching that strongly limits the efficiency and limits the maximum Erbium concentration [36]. Although in Thulium doped fibers coupling between neighboring ions is desired to achieve the so-called "2 for 1 photon effect" leading to efficient laser conversion, there exist limitations to the maximum Thulium concentration in the fiber. In order to incorporate homogeneously Thulium ion, silica fiber is also doped with a large quantity of Aluminum. The typical ratio of concentration is Al/Tm = 10 [37]. Aluminum incorporation strongly increases the core NA and can affect the glass stability. The commercial fiber with the highest Erbium concentration to our knowledge is estimated from absorption to 3.3×10^{25} ions/m^3 in an Erbium–Ytterbium co-doped fiber. We note that such a large Erbium concentration in silica only leads to efficient fibers when the fiber is co-doped. Similarly the Tm^{3+}-doped fiber with the highest concentration has an estimated concentration to 4.8×10^{26} ions/m^3. Using these highly doped fibers leads to reach the maximum gain that can be achieved with the minimum fiber length with a doped fiber amplifier. This is limited by ASE saturation to 30–40 dB.

The spectroscopic differences between Thulium and Erbium lead to large differences in the saturation power that strongly affect the ratio r through Eq. (4a). Indeed the excited state lifetime is 10 ms for Erbium whereas the fluorescence lifetime is only 350–500 μs for Thulium [38] into silica fibers. The sum of the

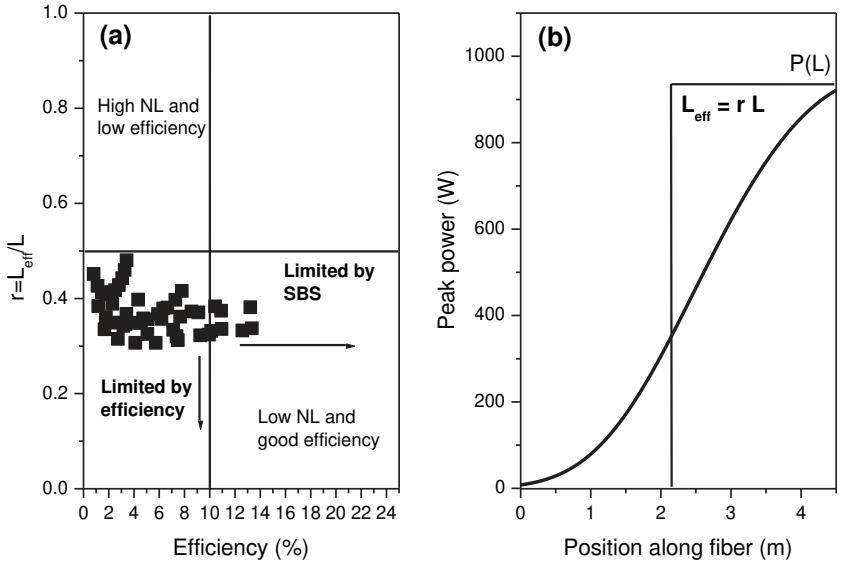

Fig. 12. (a) Modeling results of the variation of $r = L_{eff}/L$ for various input peak power and pump power fiber amplifiers based on the Thulium doped fiber (cf. Table 1) as a function of the efficiency (output average power divided by input pump power) achieved for various fiber lengths, (b) chart showing an example of the power distribution in the Thulium doped fiber amplifier.

absorption and emission cross-section in the middle of the emission band is 7×10^{-25} m^2 for Erbium at 1550 nm whereas it is 1.5×10^{-25} m^2 at 2000 nm for Thulium. The saturation power is thus 1.8 mW for an Erbium doped fiber with 100 μm^2 doped surface whereas it reaches 179 mW for a Thulium doped fiber with 100 μm^2 doped surface. This means that the exponential growth of the input power in a fiber amplifier is maintained on a longer distance in Thulium doped fiber than in Erbium doped fibers. This will decrease the ratio r and increase somewhat the SBS threshold. Conversely the saturation is more difficult to reach in Thulium doped fiber amplifiers.

To be more quantitative we have compiled on graphs the results from modeling in pulsed regime of fiber amplifiers similar to the amplifiers described in Sections 2 and 3 operated with 100 ns pulses at 20 kHz PRF for various pump and input powers. For a given pump power and signal input peak power, the population equations and the propagation equation of powers in the fiber amplifier are solved providing the power distribution $P(z,t)$. We compute the effective length from the power distribution at the time at which the pulse power at the fiber output reaches its maximum. The pulse energy is used to compute the amplifier efficiency with respect to the coupled pump power. We only plot configurations below the SBS threshold. The Brillouin gain value used to estimate the threshold are the values in Table 1 and discussed in Section 7. We assumed that external Brillouin mitigation techniques can be used to increase the SBS threshold by a factor 2.5. These techniques are usually based on temperature gradient or strain gradient as in Sections 4 and 5. For a given input peak power and pump power, when the fiber length is varied a curve in the efficiency/r ratio can be drawn. The optimal amplifier would operate in the high efficiency and small r region. However going to low r is done at the expense of efficiency and going to large efficiency leads to reach the SBS threshold. For a given fiber there is thus a limit in terms of r ratio and efficiency that can be reached. This is illustrated on Fig. 12(a) for the Tm^{3+}-doped amplifier. For $r = 0.38$ and an efficiency of 13% an optimum is reached with 1450 W peak power. Another one is $r = 0.36$ and efficiency of 13% where the peak power reaches 1700 W peak power.

We can now plot on the same chart the results obtained for the Er^{3+}–Yb^{3+} co-doped fiber amplifier (operated at 1545 nm) and the Tm^{3+} doped fiber amplifier (operated at 2050 nm) for various pump power and peak power at the optimum fiber length. The results are shown on Fig. 13.

We can see that the Erbium–Ytterbium codoped fiber amplifier always yields r ratio larger than 0.5 and almost independent on the efficiency. On the contrary the effective length of the Thulium doped fiber amplifier is decreasing for increasing pump power down to 0.3. This is a 40% difference that explains together with the Brillouin gain difference discussed in Section 7 why

Table 1
Fiber parameters used for the modeling.

Fiber doping type	Erbium/Ytterbium	Thulium
Fiber length	1.0 m	2.5 m
Core diameter	25 μm	25 μm
Mode effective area	327 μm^2	396 μm^2
Brillouin gain	1.2×10^{-11} m/W	0.9×10^{-11} m/W

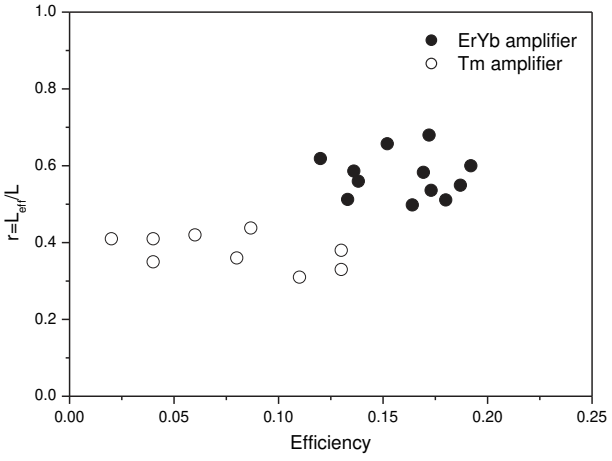

Fig. 13. Modeling results of the variation of $r = L_{eff}/L$ for various input peak power and pump power fiber amplifiers based on the Erbium–Ytterbium co-doped fiber (full disks) and Thulium doped fiber (open disks) (cf. Table 1) as a function of the efficiency achieved for the lengths indicated in Table 1.

comparable peak power can be achieved in the Thulium doped and Erbium–Ytterbium co-doped fiber amplifier whereas the fiber length used in the first case is more than 2.5 times the length of the second one. This fact is illustrated on Fig. 14 showing the maximum peak power obtained (limited either by gain or by SBS threshold).

All these discussions also apply to the short pulse amplification issue of Section 5 except that there is no threshold in that case but rather a maximum B value that we need to fix. Eq. (4b) shows the general shape of Fig. 10 with linear relation between the output energy and B-integral. More precisely we show in Appendix A that the B-integral for large gain can be written as:

$$B = \frac{gL}{A_{eff}} \frac{P(L)}{\ln\frac{P(L)}{P(0)} + \frac{P(L)}{P_{sat}}} \left[1 + \frac{1}{2}\frac{P(L)}{P_{sat}}\right] \tag{5}$$

This equation has a logarithmic term at the denominator explaining the saturating shape of the B-integral on Fig. 10 for low input energy.

With Eq. (4a) we have illustrated the trade-off between low nonlinearity and efficiency. We have used this framework to discuss the influence of spectroscopy on the differences in effective length for Erbium–Ytterbium co-doped and Thulium doped fiber amplifiers.

7. Comparison of Brillouin properties

After this discussion about the value of L_{eff} in the fiber amplifiers, we have to discuss about the value of the Brillouin gain. The Brillouin gain is a function of the material density, the Pockels coefficient, the acoustic velocity in the material and its viscosity. An interesting discussion of values of g_B as a function of materials can be found for Ytterbium doped fibers in [39]. This paper compares the Brillouin gain value for various Ytterbium doping concentrations in phosphosilicate (representative of Erbium–Ytterbium codoped fiber glass composition) and aluminosilicate (representative of Thulium doped fibers). Ytterbium has the interesting property that should be shared with other lanthanides that the Pockels coefficient is negative. This translates into a reduction of the Brillouin gain for increasing rare-earth concentrations. As a first estimate we will consider that Erbium, Ytterbium and Thulium behave in the same manner with respect to the Brillouin gain variation and use the Figs. 3 and 4 in Ref. [39].

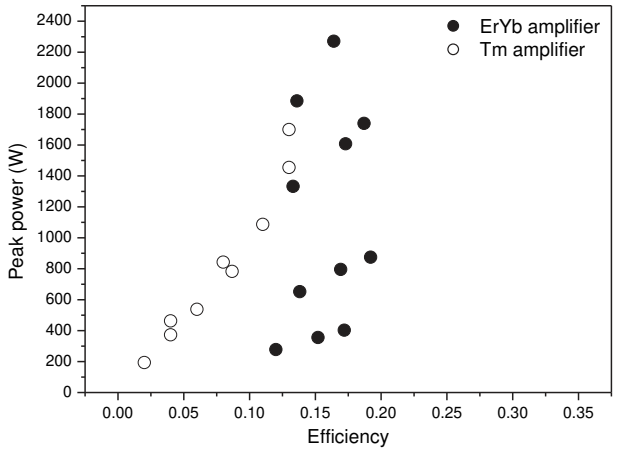

Fig. 14. Modeling results of the variation of output peak power for various input peak power and pump power fiber amplifiers based on the Erbium–Ytterbium codoped fiber (full disks) and Thulium doped fiber (open disks) (cf. Table 1) as a function of the efficiency achieved for various fiber lengths.

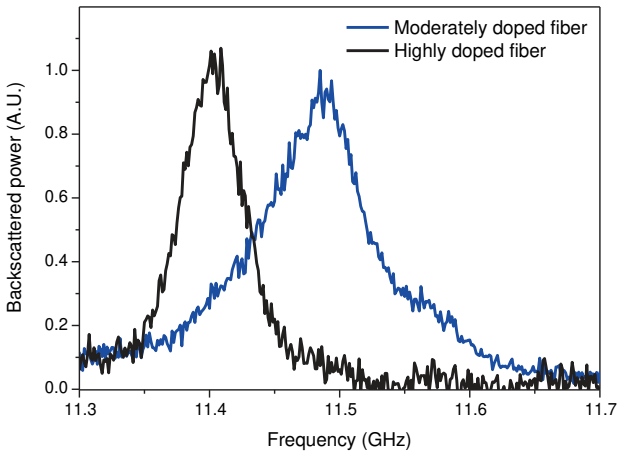

Fig. 15. Brillouin Backscattered light from two Tm^{3+} doped fibers with different doping level measured at 1545 nm.

Erbium–Ytterbium codoped fibers are heavily doped with phosphorous to decrease the $^4I_{11/2}$ lifetime. The typical concentration that we will assume is 10 mol% P_2O_5 for 1 mol% Ytterbium. This should result in $g_B \sim 0.7 \times 10^{-11}$ m/W for a bulk material. The effective value of the Brillouin gain is affected by the radial distribution of the dopants. The calculation taking a typical Phosphosilicate profile gives $g_B \sim 1.2 \times 10^{-11}$ m/W.

Thulium doped fibers are heavily doped with alumina to prevent Tm^{3+} cluster formations. Typically the Aluminum concentration is 10 times larger than Thulium concentration. We expect in the LMA fiber of Section 4 to have 4.6 mol% Aluminum for 0.46 mol% Thulium. This should result in $g_B \sim 0.9 \times 10^{-11}$ m/W. Note that we have also estimated for another fiber less doped $g_B \sim 1.2 \times 10^{-11}$ m/W.

The value of the Brillouin gain that we have discussed so far is the Brillouin gain value obtained for a homogenous fiber length L. Among the various methods used to increase the Brillouin threshold several are based on strain [15,25] or temperature [40–42] change along the fiber. The principle is to shift the Brillouin gain maximum along the fiber. The Brillouin threshold increases as a function of the ratio of the total induced shift over the fiber length to the Brillouin spontaneous linewidth [14].

We have measured by the heterodyne technique the spectrum of the backscattered Stokes light blow threshold on a Tm^{3+} doped fiber with moderate doping (core absorption at 1650 nm is 80 dB/m). As we had not access to a high speed and high sensitivity photodetector for the 2 μm band, we used a 1545 nm laser amplified to 2 W CW. The spectrum appears to have one broad peak centered at 11.489 GHz with a full width at half maximum of 95 MHz (see Fig. 15). The same setup was used to measure a highly Tm^{3+} doped fiber (core absorption at 1650 nm is 350 dB/m). For this fiber the peak is centered at 11.403 GHz with a full width at half maximum of 61 MHz. This is for the best our knowledge the first measurement of the Brillouin spectrum of a Thulium doped fiber.

This width is larger than the width measured at 1545 nm on several Erbium–Ytterbium co-doped fibers (typically 50 MHz) [41] or Ytterbium doped fibers (typically 50 MHz) [39] and much larger than the width we measured on the standard SMF28 fiber (30 MHz). This can be explained by the presence of a large quantity of alumina in highly Tm^{3+}-doped fibers [39]. In order to compute the Brillouin width for 2050 nm, we can use the $1/\lambda^2$ scaling law of the Brillouin linewidth with wavelength [9]. For the highly doped fiber the corresponding width would then be 28 MHz at 2050 nm.

This short study shows that the Brillouin gain in Tm^{3+} doped fiber will be about 30% smaller than in Erbium–Ytterbium codoped

fiber. Assuming that the highly doped fiber is representative of the Tm^{3+} doped fibers, Brillouin linewidth at given wavelength are comparable for Erbium–Ytterbium codoped and Thulium doped fibers. The $1/\lambda^2$ scaling of the linewidth and $1/\lambda$ scaling of the Brillouin shift would then make the external mitigation techniques about 30% more efficient at 2050 nm.

8. Conclusions

We have reviewed the design and performances of several pulsed eyesafe MOPFA operating either at 1.5 μm or 2 μm. At 1545 nm a single-frequency MOPFA based on LMA Erbium–Ytterbium codoped has generated up to 630 W peak power single frequency. At 2050 nm a MOPFA based on LMA Thulium doped fibers has generated up to 1 kW peak power single frequency. To the best our knowledge this is the highest peak power for single-frequency 100 ns pulses beyond 2000 nm. At 1960 nm a MOPFA based on single mode Thulium doped fibers has generated 26 nJ with 3 ps pulses for a B integral of $\pi/2$.

A new framework to analyze the effective length variation with the design parameters of a fiber amplifier has been proposed. It clearly shows the role of the saturation power. Finally we have compared the Brillouin gain properties of Erbium–Ytterbium codoped fibers to Thulium doped fibers. The spectrum of Thulium doped fibers was reported for the first time. We measured a linewidth of 61–95 MHz (at 1545 nm) depending on the fiber.

Acknowledgments

Authors would like to acknowledge for fundings: the European Commission with UFO Project (Project Grand Agreement 314237); Region Ile-de-France with SOLAIRE Project; Agence Nationale de la Recherche with CONFIAN Project; Conseil général de l'Essonne with MUSEON Project and Keopsys for PhD funding.

Appendix A. Appendix A

We start from the propagation equation in continuous wave regime of power $P(z)$ in a saturating medium with small signal gain g_0 and saturation power P_{sat}.

$$\frac{\partial P}{\partial z} = \frac{g_0}{1+\frac{P}{P_{sat}}}P \tag{A.1}$$

Now let us consider the effective length

$$L_{eff} = \frac{1}{P(L)}\int_0^L P(z)dz \tag{A.2}$$

Assuming that the signal distribution is monotonous over the fiber which should be the case in the absence of reabsorption we can make a change of variables. Using Eq. (A.1) we get:

$$L_{eff} = \frac{1}{P(L)}\int_{P(0)}^{P(L)} \frac{1+x/P_{sat}}{g_0}dx \tag{A.3}$$

Eq. (A.3) can then be integrated leading to the following expression introducing the total amplifier gain $G_A = P(L)/P(0)$:

$$L_{eff} = \frac{1}{g_0}\left[1 - G_A^{-1} + \frac{(1-G_A^{-2})}{2}\frac{P(L)}{P_{sat}}\right] \tag{A.4}$$

Integration of (A.1) over the fiber length leads to:

$$\ln G_A = g_0 L - \frac{P(L)}{P_{sat}}(1-G_A^{-1}) \tag{A.5}$$

Combining (A.4) and (A.5) we find:

$$L_{eff} = \frac{1}{\ln G_A + \frac{P(L)}{P_{sat}}(1-G_A^{-1})}\left[1 - G_A^{-1} + \frac{(1-G_A^{-2})}{2}\frac{P(L)}{P_{sat}}\right]$$

In the limit of large gain G_A we get:

$$L_{eff} = \frac{L}{\ln\frac{P(L)}{P(0)} + \frac{P(L)}{P_{sat}}}\left[1 + \frac{1}{2}\frac{P(L)}{P_{sat}}\right] \tag{A.6}$$

or

$$L_{eff} = \frac{1}{g_0}\left[1 + \frac{1}{2}\frac{P(L)}{P_{sat}}\right] \tag{A.7}$$

Eq. (A.6) leads to the expression for the B integral:

$$B = \frac{gL}{A_{eff}}\frac{P(L)}{\ln\frac{P(L)}{P(0)} + \frac{P(L)}{P_{sat}}}\left[1 + \frac{1}{2}\frac{P(L)}{P_{sat}}\right] \tag{A.8}$$

The logarithmic term in (A.8) ratio explains the saturating behaviour of B integral in Fig. 10 for low input power (large gain).

We can finally see when starting back from Eq. (A.1) that for $P(z) \gg P_{sat}$, the power growth is linear leading to $L_{eff} = L/2$.

References

[1] G. Canat, Y. Jaouen, J.-C. Mollier, Performance and limitations of high brightness Er3+/Yb3+ fiber sources, C.R. Phys. 7 (2) (2006) 177–187.
[2] G. Sefler, W. Mack, G. Valley, T. Rose, Secondary energy transfer and nonparticipatory Yb3+ ions in Er3+–Yb3+ high-power amplifier fibers, J. Opt. Soc. Am. B 21 (10) (2004) 1740–1748.
[3] G. Canat, J. Mollier, J. Bouzinac, G. Williams, B. Cole, L. Goldberg, G. Kulcsar, Y. Jaouën, Power limitations of fiber lasers at 1.5 ìm by parasitic lasing effects, in: Conference on Lasers and Electro-Optics/International Quantum Electronics Conference and Photonic Applications Systems Technologies, Technical Digest (CD), Optical Society of America, 2004. Paper CMK6.
[4] S.D. Jackson, S. Mossman, Efficiency dependence on the Tm^{3+} and Al^{3+} concentrations for Tm^{3+}-doped silica double-clad fiber lasers, Appl. Opt. 42 (15) (2003) 2702–2706.
[5] M. Broer, D. Krol, D. DiGiovanni, Highly nonlinear near-resonant photodarkening in a thulium-doped aluminosilicate glass fiber, Opt. Lett. 18 (10) (1993) 799–801.
[6] Y. Jaouen, G. Canat, S. Grot, S. Bordais, Power limitation induced by nonlinear effects in pulsed high-power fiber amplifiers, C.R. Phys. 7 (2006) 163–169.
[7] S. Le Floch, P. Cambon, Theoretical evaluation of the Brillouin threshold and the steady-state Brillouin equations in standard single-mode optical fibers, J. Opt. Soc. Am. A 20 (6) (2003) 1132–1137.
[8] G. Kulcsar, Y. Jaouen, G. Canat, E. Olmedo, G. Debarge, Multiple-stokes stimulated Brillouin scattering generation in pulsed high-power double-cladding Er^{3+}–Yb^{3+} codoped fiber amplifier, Photonics Technol. Lett. IEEE 15 (6) (2003) 801–803.
[9] G.P. Agrawal, Nonlinear Fiber Optics, 4th ed., Academic, 2007.
[10] J.-P. Cariou, B. Augère, M. Valla, Laser source requirements for coherent lidars based on fiber technology, C.R. Phys. 7 (2006).
[11] L. Gruner-Nielsen, D. Jakobsen, S. Herstrom, B. Palsdottir, S. Dasgupta, D. Richardson, P. Andrekson, Brillouin suppressed in highly nonlinear fibers, in: Optical Communications (ECOC), 38th European Conference and Exhibition on IEEE (2012) 1–3.
[12] G. Canat, S. Jetschke, S. Unger, L. Lombard, P. Bourdon, J. Kirchhof, V. Jolivet, A. Dolfi, O. Vasseur, Multifilament-core fibers for high energy pulse amplification at 1.5 μm with excellent beam quality, Opt. Lett. 33 (22) (2008) 2701–2703.
[13] Y.W. Lee, K.E. Urbanek, M.J.F. Digonnet, R.L. Byer, S. Jiang, Measurement of the stimulated Brillouin scattering gain coefficient of a phosphate fiber, Proc. SPIE 6469 (2007). Optical Components and Materials IV, 64690L.
[14] J. Boggio, J. Marconi, H. Fragnito, Experimental and numerical investigation of the SBS-threshold increase in an optical fiber by applying strain distributions, J. Lightwave Technol. 23 (11) (2005) 3808–3814.
[15] X. Zhang, W. Diao, Y. Liu, J. Liu, X. Hou, W. Chen, Single-frequency polarized eye-safe all-fiber laser with peak power over kilowatt, Appl. Phys. B 115 (1) (2013) 123–127.
[16] M. Akbulut, J. Hwang, F. Kimpel, S. Gupta, H. Verdun, Pulsed coherent fiber lidar transceiver for aircraft in-flight turbulence and wake-vortex hazard detection, Proc. SPIE 8037 (2011). Laser Radar Technology and Applications XVI, 80370R.
[17] W. Renard, D. Goular, M. Valla, C. Planchat, B. Augère, A. Dolfi-Bouteyre, C. Besson, G. Canat. Beyond 10 Km range wind-speed measurement with a 1.5 μm all-fiber laser source, accepted for CLEO, 2014.
[18] G.G. Vienne, J.E. Caplen, L. Dong, J.D. Minelly, J. Nilsson, D.N. Payne, Fabrication and characterization of Er3+/Yb3+: phosphosilicate fibers for lasers, J. Lightwave Technol. 16 (11) (1998) 1990–2001.

[19] A. Malinowski, K.T. Vu, K.K. Chen, J. Nilsson, Y. Jeong, S. Alam, D. Richardson, High power pulsed fiber MOPA system incorporating electro-optic modulator based adaptive pulse shaping, Opt. Express 17 (23) (2009) 20927–20937.
[20] Q. Fang, W. Shi, E. Persen, K. Kieu, A. Chavez-Pirson, N. Peyghambarian, Half-mJ all-fiber-based single-frequency nanosecond pulsed fiber laser at 2 μm, Photonics Technol. Lett. IEEE 24 (5) (2012) 353–355.
[21] W. Shi, E. Petersen, D. Nguyen, Z. Yao, A. Chavez-Pirson, N. Peyghambarian, J. Yu, 220 μJ monolithic single-frequency Q-switched fiber laser at 2 μm by using highly Tm^{3+}-doped germanate fibers, Opt. Lett. 36 (2011) 3575–3577.
[22] G.D. Goodno, L.D. Book, J. Rothenberg, Low-phase-noise, single-frequency, single-mode 608 W thulium fiber amplifier, Opt. Lett. 34 (8) (2009) 1204–1206.
[23] D. Creeden, P.A. Budni, P.A. Ketteridge, Pulsed Tm-doped fiber lasers for mid-IR frequency conversion, Proc. SPIE 7195 (2009) 1.
[24] A. Godard, Infrared (2–12 μm) solid-state laser sources: a review, C.R. Phys. 8 (2007) 1100.
[25] E. Lucas, G. Canat, L. Lombard, Y. Jaouën, S. Bordais, 1 kW peak power 110 ns single-frequency Thulium doped fiber amplifier at 2050 nm, Appl. Opt. (2014). article submitted 18th of February.
[26] S.D. Jackson, T.A. King, Theoretical modelling of Tm-doped silica fiber lasers, J. Lightwave Technol. 17 (5) (1999) 948–956.
[27] D. Creeden, B.R. Johnson, S.D. Setzler, E.P. Chicklis, Resonantly pumped Tm-doped fiber laser with >90% slope efficiency, Opt. Lett. 39 (I) (2014) 470–473.
[28] S.D. Jackson, A. Sabella, D.G. Lancaster, Application and development of high-power and highly efficient silica-based fiber lasers operating at 2 μm, J. Sel. Top. Quantum Electron. 13 (3) (2007) 567–572.
[29] W. Renard, G. Canat, P. Bourdon, 26 nJ picosecond solitons from thulium-doped single-mode master oscillator power fiber amplifier, Opt. Lett. 37 (I) (2012) 377–379.
[30] Advanced Solid-State Photonics, OSA Technical Digest Series (CD), Optical Society of America, 2010. Paper AMB10.
[31] R.A. Sims, P. Kadwani, L. Shah, M. Richardson, Generation and amplification of 350 fs, 2 μm pulses in Tm:fiber, Proc. SPIE 7914 (2011) 79141L.
[32] F. Haxsen, D. Wandt, U. Morgner, J. Neumann, D. Kracht, Pulse energy of 151 nJ from ultrafast thulium-doped chirped-pulse fiber amplifier, Opt. Lett. 35 (17) (2010) 2991–2993.
[33] M. Perry, T. Ditmire, B. Stuart, Self-phase modulation in chirped pulse amplification, Opt. Lett. 19 (24) (1994) 2149–2151.
[34] E. Lucas, L. Lombard, G. Canat, Dépendance en température d'un amplificateur à fibre dopée thulium pompé à 1560 nm, J. Natl. Opt. Guidée (2012).
[35] W. Renard, G. Canat, P. Bourdon, All thulium fiber single-mode master oscillator power amplifier delivering 32-nJ picosecond pulses, Proc. SPIE 8237 (2012). Fiber Lasers IX: Technology, Systems, and Applications, 82372N.
[36] P. Myslinski, D. Nguyen, J. Chrostowski, Effects of concentration on the performance of erbium-doped fiber amplifiers, J. Lightwave Technol. 15 (1) (1997) 112–120.
[37] S.D. Jackson, Cross relaxation and energy transfer upconversion processes relevant to the functioning of 2 μm Tm3+-doped silica fibre lasers, Opt. Commun. 230 (1) (2004) 197–203.
[38] P.F. Moulton, G.A. Rines, E.V. Slobodtchikov, K.F. Wall, G. Frith, B. Samson, A.L. Carter, Tm-doped fiber lasers: fundamentals and power scaling, Sel. Top. Quantum Electron. 15 (1) (2009) 85–92.
[39] P.D. Dragic, J. Ballato, S. Morris, T. Hawkins, The Brillouin gain coefficient of Yb-doped aluminosilicate glass optical fibers, Opt. Mater. 35 (9) (2013) 1627–1632.
[40] G.D. Goodno, L.D. Book, J.E. Rothenberg, M.E. Weber, S.S. Benjamin, Weiss; narrow linewidth power scaling and phase stabilization of 2-μm thulium fiber lasers, Opt. Eng. 50 (11) (2011) 111608.
[41] G. Canat, A. Durécu, G. Lesueur, L. Lombard, P. Bourdon, V. Jolivet, Y. Jaouën, Characteristics of the Brillouin spectra in Erbium–Ytterbium fibers, Opt. Express 16 (5) (2008) 3212–3222.
[42] V. Kovalev, R. Harrison, Suppression of stimulated Brillouin scattering in high-power single-frequency fiber amplifiers, Opt. Lett. 31 (2006) 161–163.